High-Power Density Wound-Field Flux-Switching Machine with Modular Rotor Design for Traction Applications

Mostafa Fereydoonian
Elmore Family School of Electrical and Computer Engineering
Purdue University
West Lafayette, IN, USA
mostafaf@purdue.edu

Woongkul Lee
Elmore Family School of Electrical and Computer Engineering
Purdue University
West Lafayette, IN, USA
lee5279@purdue.edu

Abstract—This paper investigates the electromagnetic performance of a wound-field flux-switching machine (WFFSM) with a new modular rotor design. The WFFSMs have both windings on the stator with inefficient magnetic flux paths that do not directly contribute to torque generation. Moreover, due to the flux switching in the rotor, the rotor core loss of flux-switching machines (FSMs) is generally higher than that of the regular externally excited synchronous machines (EESMs), which will degrade the efficiency of FSMs. The rotor geometry plays a crucial role in influencing the flux linkage between field and armature windings and, consequently, the electromagnetic performance. Therefore, the primary objective of this paper is to design a novel modular rotor design that facilitates an optimal magnetic flux path, leading to higher torque, lower core loss, and higher efficiency. The result shows the new modular rotor topology significantly reduces core loss while enhancing torque and efficiency. In the case of toroidal winding WFFSM, core loss decreased by 27%, with torque and efficiency increasing by 9% and 1.7%, respectively.

Keywords— Circumferential winding, externally excited synchronous machine, flux-switching machine, high-power density, modular rotor, segmented rotor, toroidal winding.

I. INTRODUCTION

The race is on to reduce reliance on electric vehicle (EV) motor magnets made from rare earth elements (RE). RE magnets are crucial components in the most efficient torque and power-dense motors used in EVs. However, concerns about cost, sustainability, and geopolitical vulnerabilities in the supply chain have prompted governmental bodies and the industry to explore alternative motor technologies. As of 2020, approximately 77% of the propulsion motors in plug-in hybrid electric vehicles (PHEVs) and battery electric vehicles (BEVs) were permanent magnet (PM) machines, with the remainder divided between magnet-free induction machines at 17% and externally excited synchronous machines (EESMs) at 6% [1].

Wound-field flux-switching machines (WFFSMs) are a type of EESMs where both field and armature windings are located on the stator. This design eliminates the need for brushes and slip rings, as illustrated in Fig. 1. Two possible winding topologies (i.e., circumferential and toroidal) exist for the field and armature windings. Therefore, based on winding topology, there are two types of WFFSMs: circumferential winding (CW) and toroidal winding (TW). In TW WFFSM, field and armature windings are wound around the stator yoke instead of stator teeth. This type of stator design is relatively easy to manufacture with a higher winding fill factor, and it provides better cooling because the stator winding is directly exposed to the stator housing with a cooling jacket. However, both field and armature windings coexist in the stator, leading to a complex and inefficient magnetic flux path generation resulting in harmonic components in terminal voltage and inductance [2]-[3]. Moreover, due to the flux switching in the rotor, the rotor core loss of flux-switching machines (FSMs) is much more than that of the regular EESMs, which will degrade the efficiency of FSMs [4]. These issues in WFFSM cause the machine core to become more saturated as the current density increases without significantly boosting power density. This problem statement has thus initiated further research into designing a new motor topology that enhances the power density and efficiency of the WFFSM.

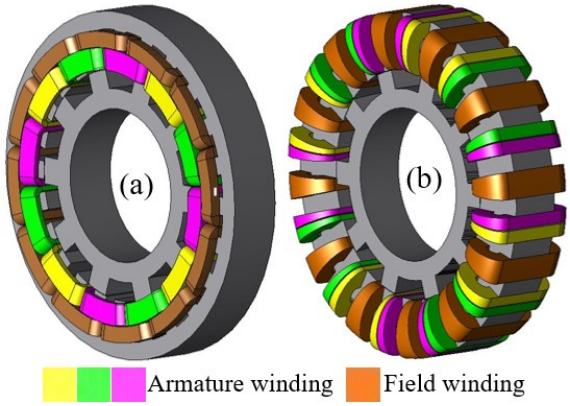

Fig. 1. 3D view of (a) CW WFFSM (b) TW WFFSM.

The torque production mechanism of WFFSMs is investigated in [5] and [6]. The studies in [7]-[8] demonstrate that adding an asymmetric flux barrier in the rotor structure can effectively align the reluctance torque component with the peak magnet torque, thereby enhancing power density. The study in [9] proposed a dual-rotor WFFSM topology with an air-core stator employing superconducting technology to markedly enhance power density and efficiency. The study in [10] presents a rotor saliency optimization for TW WFFSM to

TABLE 1. WOUND-FIELD FLUX-SWITCHING MACHINE SPECIFICATION.

Parameter	Units	Value
Rated Speed	rpm	4,000
Stator/rotor pole	-	12/10
DC current density (J_{dc})	A/mm^2	8.5
AC current density (J_{ac})	A/mm^2	8.5
N_{dc} (turns per dc coil)	-	4
N_{ac} (turns per coil per phase)	-	3
Stator outer diameter	mm	540
Rotor outer diameter	mm	359
Stator tooth width	mm	28
Rotor tooth width	mm	42
Fill factor	-	0.5
Air gap length (l_g)	mm	0.5
Stack length	mm	80
Lamination thickness	mm	0.35

mitigate higher-order special harmonic components in terminal voltage and inductance, improving the overall electromagnetic performance. The problem with this method is the rotor saliency optimization increases the average airgap length, leading to lower torque. To bridge the knowledge gap in high-power density WFFSM design, this paper proposes a modular rotor design, which has great potential to eliminate the longer magnetic flux path issue while increasing the average output torque, decreasing the core loss, and improving the efficiency. The results reveal that among various WFFSM topologies, the modular rotor design stands out as a promising candidate for significantly enhancing power density and efficiency by increasing the current density to higher levels.

This paper is outlined as follows. Section II investigates the magnetic flux path and terminal voltage of WFFSM. Torque segregation was carried out to highlight the effects of integrated stator structure on output torque. Section III presents the modular rotor topology for both TW and CW WFFSMs, investigating the impact of flux barrier insertion on the magnetic flux path. It investigates how the new modular rotor design affects electromagnetic performance in metrics including terminal voltage, output torque, and core loss. Section IV will present and discuss the new rotor design results. Finally, the conclusion summarizes the essential results.

II. WOUND-FIELD FLUX-SWITCHING MACHINE MAGNETIC FLUX PATH ANALYSIS

The comparative study in this paper selects one of the most viable stator/rotor pole combinations, 12/10 FSMs for electric propulsion applications. All WFFSMs under study are 12/10 configuration with the same materials and dimensions, as summarized in Table 1. It should be noted that all the analyses in this paper assume that the rotor is rotating in a counterclockwise direction and that the machine is under motoring operation.

In CW WFFSM, field and armature windings are wound around the stator teeth. The rotor has a typical toothed shape structure, as shown in Fig. 2. In TW WFFSM, field, and armature windings are wound around the stator yoke instead of the stator teeth. The rotor has a typical toothed shape structure, as depicted in Fig. 3. This type of stator winding has the advantages of short end-winding and no winding overlap. It is

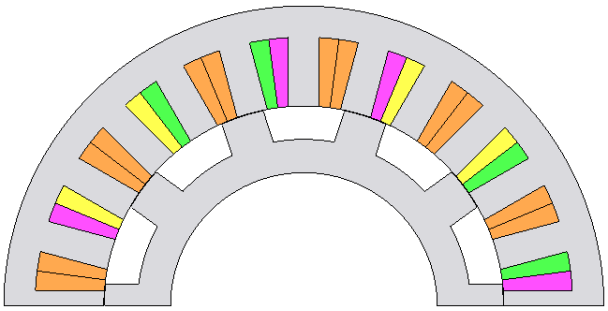

Fig. 2. 2D view of toothed rotor CW WFFSM

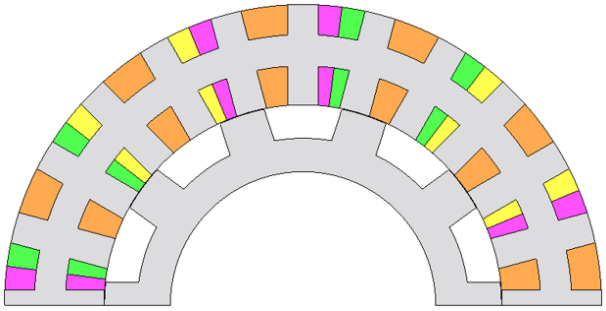

Fig. 3. 2D view of toothed rotor TW WFFSM

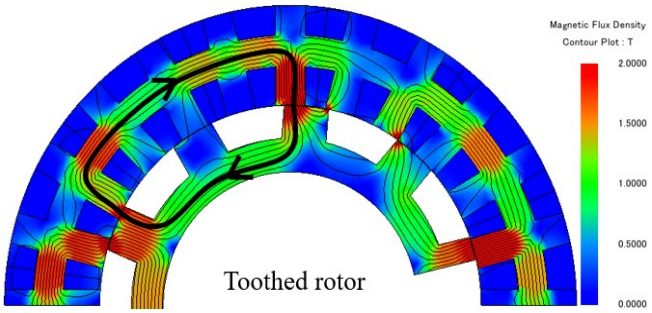

Fig. 4. Toothed rotor TW WFFSM magnetic flux density and magnetic flux line (@ J_{dc} = 8.5 A/mm^2, J_{ac} = 8.5 A/mm^2).

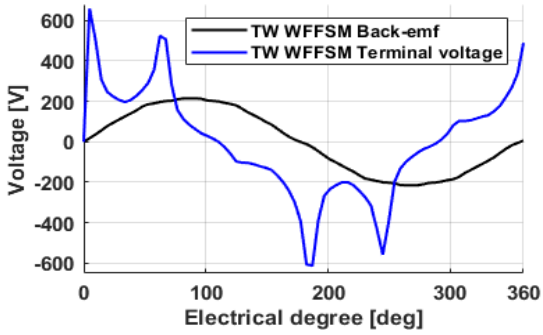

Fig. 5. Toothed rotor TW WFFSM back-emf and terminal voltage (@ J_{ac} = 8.5 A/mm^2) waveforms.

relatively easy to manufacture with a higher fill factor [11]. It also provides better cooling because the stator windings are directly exposed to the stator housing with a cooling jacket [12]. The integrated stator structure in WFFSM leads to longer magnetic flux paths between phases. It generates localized saturation regions in the stator poles and back iron, as illustrated in Fig. 4. This longer magnetic flux path at some specific rotor positions increases armature winding self- and mutual inductances, generates negative reluctance torque, and consequently decreases the net output torque [3], [10].

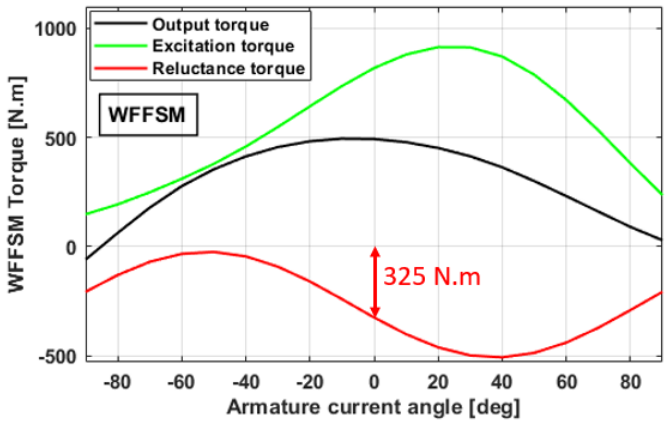

Fig. 6. WFFSM torque segregation (@ J_{dc} = 8.5 A/mm^2, J_{ac} = 8.5 A/mm^2).

The terminal voltage waveform and the corresponding back-emf waveform of the toothed rotor TW WFFSM are depicted in Fig. 5. This machine exhibits a sinusoidal back-emf waveform with rms values of 151 V. However, in one electric cycle, its terminal voltage shows four spikes up to 660 V. These spatial harmonics come from the integrated stator structure in WFFSMs [3]. Assuming armature winding resistance is relatively small and terminal voltage is equal to the derivative of its flux linkage. This means that four specific rotor positions create a longer magnetic flux path during an electric cycle. This leads to a steep change in the armature winding flux linkage, producing four spikes in the terminal voltage waveforms.

Torque segregation is carried out to highlight the effects of integrated stator structure on self- and mutual inductances and, consequently, output torque. An FEA-based frozen permeability method is used to segregate the torque components. The torque components of TW WFFSM, including excitation torque, reluctance torque, and net output torque, are plotted as functions of the armature current phase angle in Fig. 6. The plot provides a visual representation of the variations in torque components for different armature current phase angles. The WFFSM generates a significant negative reluctance torque of 325 N.m at zero current phase angle, which is 39.7% of its excitation torque. This significant negative reluctance torque arises from the presence of armature winding inductance odd harmonics that adversely affect the net output torque production capability of this machine. Therefore, this torque segregation indicates that with an integrated stator structure, it is impossible to fully utilize the maximum capability of both torque components simultaneously, as they counteract each other. The primary objective of this new rotor design is to eliminate the longer magnetic flux path and shift the reluctance torque component, thereby boosting the net output torque. The subsequent sections elaborate on a new modular rotor topology.

III. WFFSMs WITH MODULAR ROTOR DESIGN

In general, FSMs are designed to have modular stators and doubly salient structures to maximize the magnetic flux density in the air gap. Furthermore, the modular stator causes the phase windings to have low mutual inductance. However, TW and CW WFFSMs have integrated stator structures, resulting in large phase winding mutual inductances. One approach is to modularize the rotor structure to maintain the modularity of the WFFSM structure. The proposed modular rotor design is illustrated in Fig. 7. A magnetic flux barrier is inserted vertically into the center of each rotor tooth, reducing the longer magnetic flux path. These barriers must not be placed in the rotor yoke between adjacent rotor teeth, as they would block the main flux path responsible for output torque. Instead, the flux barriers should be positioned centrally within each rotor tooth to guide the flux along the optimal magnetic path. The magnetic flux density and the flux path of the modular rotor design are depicted in Fig. 8. This design considerably reduces the saturated regions in both the stator yoke and poles and the rotor yoke. This implies that these flux barriers in the middle of rotor teeth prevent magnetic flux from encircling through undesirable longer paths, as depicted in Fig. 4. TW and CW WFFSMs have rotor structure duality. TW WFFSM needs a U-shape modular rotor, while CW WFFSM needs an I-shape modular rotor.

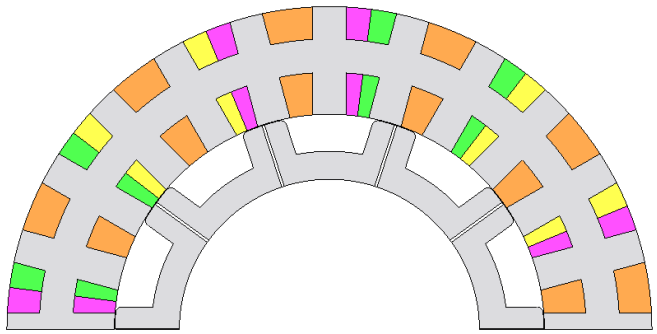

Fig. 7. 2D view of the modular rotor TW WFFSM.

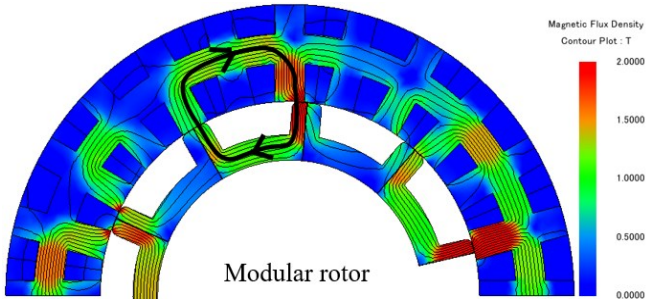

Fig. 8. The Modular rotor TW WFFSM magnetic flux density and magnetic flux line (@ J_{dc} = 8.5 A/mm^2, J_{ac} = 8.5 A/mm^2).

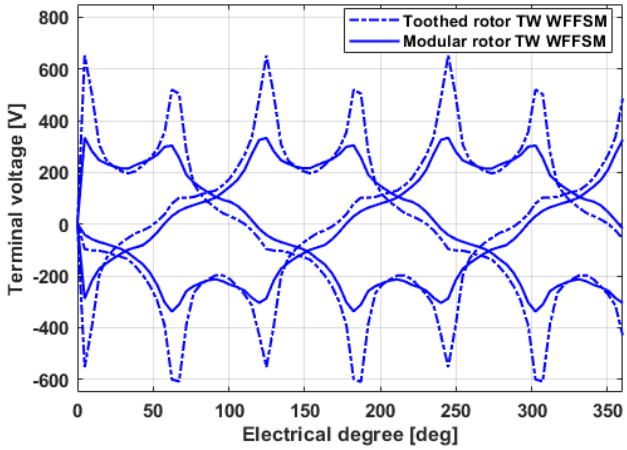

Fig. 9. Toothed and modular rotor TW WFFSMs terminal voltage (@ J_{dc} = 8.5 A/mm^2, J_{ac} = 8.5 A/mm^2).

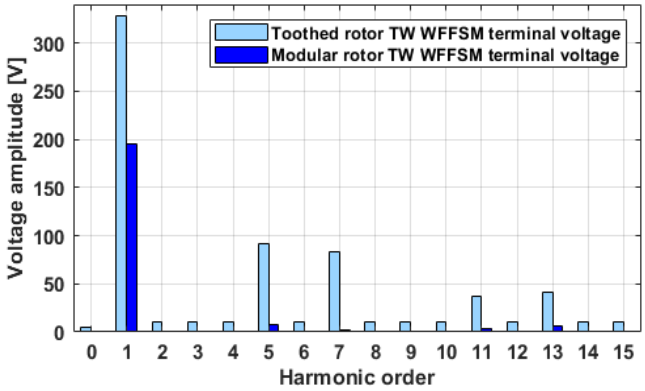

Fig. 10. Toothed and modular rotor TW WFFSMs terminal voltage harmonic content (@ J_{dc} = 8.5 A/mm^2, J_{ac} = 8.5 A/mm^2).

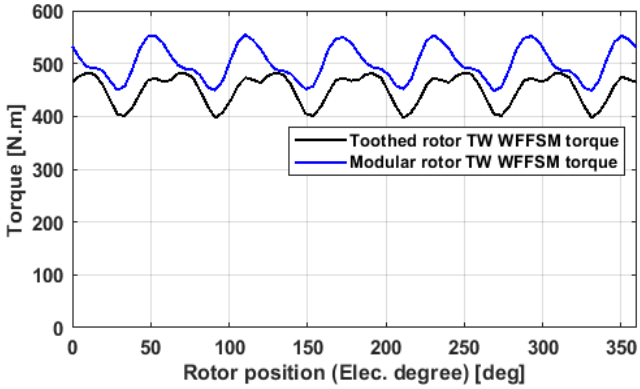

Fig. 11. Toothed rotor and modular rotor TW WFFSM instantaneous torque (@ J_{dc} = 8.5 A/mm^2, J_{ac} = 8.5 A/mm^2) waveforms for an electrical cycle.

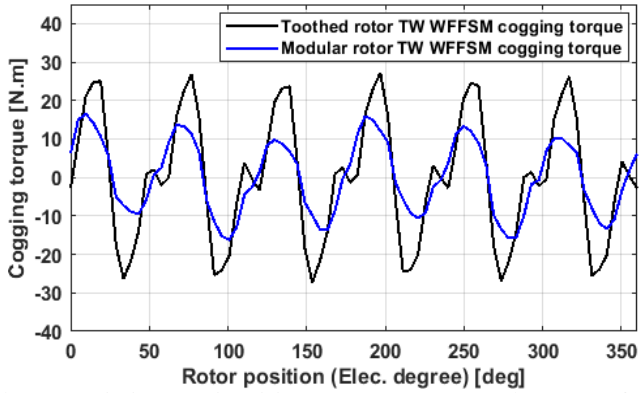

Fig. 12. Toothed rotor and modular rotor TW WFFSM cogging torque (@ J_{dc} = 8.5 A/mm^2, J_{ac} = 0 A/mm^2) waveforms for an electrical cycle.

A. Terminal Voltage

The terminal voltage waveforms of TW WFFSM in one electric cycle for both toothed and modular rotor designs is illustrated in Fig. 9. It is evident that the modular rotor design effectively reduced voltage spikes. Notably, the terminal voltage THD decreased from 46% with the toothed rotor to 16% with the modular rotor TW WFFSM. The terminal voltage spectral analysis is presented in Fig. 10. The modular rotor prominently suppressed the terminal voltage odd harmonics of the 5th, 7th, 11th, 13th. The AC-DC mutual inductance is the primary contributor to developing torque, and the self- and mutual inductances of AC winding lead to negative reluctance torque that degrades the performance of WFFSM [10].

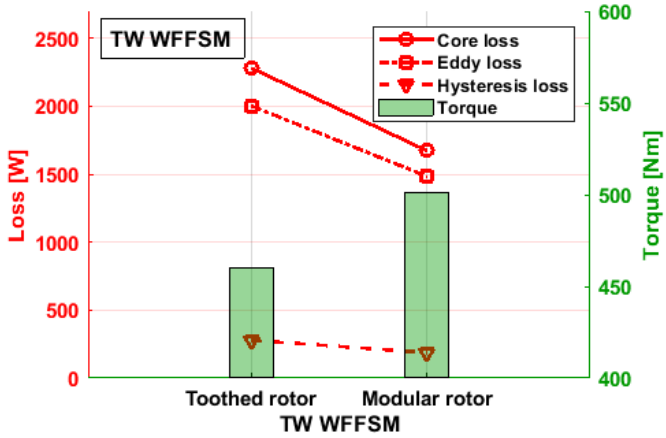

Fig. 13. Comparison of torque and losses for toothed and modular rotor TW WFFSM (@ J_{dc} = 8.5 A/mm^2, J_{ac} = 8.5 A/mm^2).

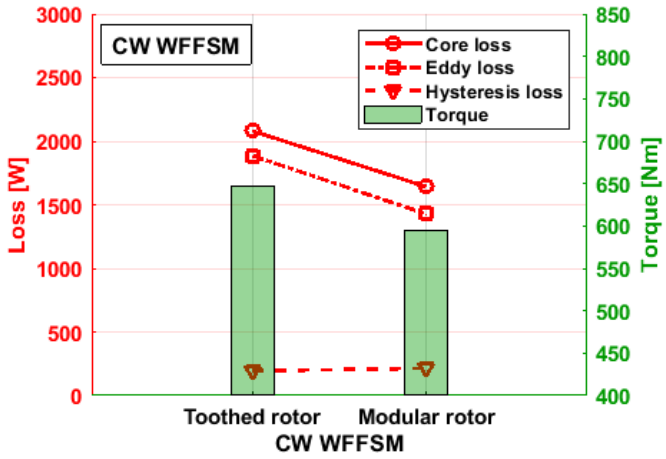

Fig. 14. Comparison of torque and losses for toothed and modular rotor CW WFFSM (@ J_{dc} = 8.5 A/mm^2, J_{ac} = 8.5 A/mm^2).

B. Torque Characteristics

The instantaneous output torque waveforms of the toothed rotor and the modular rotor TW WFFSMs are compared in Fig. 11. The toothed rotor and modular rotor have an average torque of 460 N.m and 501 N.m, respectively. Adopting flux barriers in the modular rotor topology mitigates the longer magnetic flux path issue. This reduction decreases the self- and mutual inductances of the phase windings, consequently lowering the negative reluctance torque and resulting in an overall torque increase of 9%.

The cogging torque waveforms are plotted in Fig. 12. The peak-to-peak cogging torque is reduced by 42% with modular rotor topology. Due to the stator and rotor saliency, WFFSMs often exhibit relatively high cogging torque that is proportional to the variation of field winding self-inductance. The result shows that the modular rotor design effectively reduced the variation in field winding self-inductance, consequently reducing cogging torque.

C. Core Losses

Due to the flux switching in the rotor, the rotor core loss of FSMs is much more than that of the regular EESMs, which will degrade the efficiency of FSMs [4]. A comparative analysis detailing core losses and output torque for toothed and modular rotor design is presented in Fig. 13. Besides a 9% increase in

Table 2. Comparative analysis of WFFSMs (@ j_{dc} = 8.5 A/mm^2, j_{ac} = 8.5 A/mm^2).

Type	Toothed rotor TW WFFSM	Modular rotor TW WFFSM	Toothed rotor CW WFFSM	Modular rotor CW WFFSM
Machine design	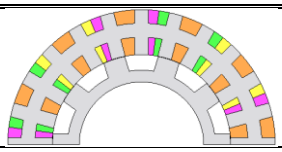	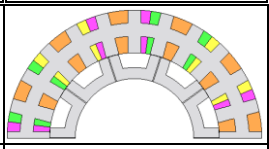	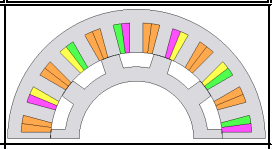	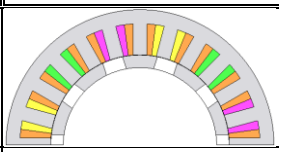
Output torque [Nm]	460	501	647	594
Cogging torque [Nm]	55	32	72	97
Torque ripple [%]	17.8	20	8	9
Terminal voltage THD [%]	46	16	6	18
Copper loss [W]	1999	1999	4600	3000
Core loss [W]	2283	1672	2080	1642
Efficiency [%]	91.5	93.2	91	93
Manufacturing consideration	✓ No winding overlaps. ✓ Short end winding. ✓ Higher filling factor. ✓ Better cooling capability. • Relatively lower efficiency. • Relatively lower power density. • Local saturation in stator poles and yoke, as well as rotor yoke. • High voltage harmonics.	✓ Highest efficiency. ✓ No winding overlaps. ✓ Short end winding. ✓ Higher filling factor. ✓ Better cooling capability. • Mechanical complexity of the rotor structure.	✓ Highest output torque. ✓ Lower torque ripple. • High cogging torque. • Lowest efficiency. • Winding overlap. • Long end-winding. • Local saturation in stator back iron and poles.	✓ Relatively high efficiency. ✓ No winding overlaps. ✓ Short end winding. ✓ Relatively lower weight. • Relatively lower torque • High cogging torque. • Mechanical complexity of the rotor structure.

output torque, the modular rotor offers an additional benefit with a notable reduction in core losses. Space harmonics (specifically the 5th, 7th, 11th, and 13th) of the air gap magnetic flux, which generates eddy and hysteresis losses, are effectively diminished. Hysteresis, eddy current, and core losses were reduced by 26%, 32%, and 27%, respectively.

Fig. 14 illustrates the output torque and core losses observed in both toothed and modular rotor CW WFFSMs. While the modular rotor design in CW WFFSM does not result in higher output torque, it significantly reduces copper loss and core losses. This design requires non-overlapped field and armature windings, as shown in Table 1. The single-tooth winding arrangement allows for potential material and energy savings by shortening the stator end windings of the modular rotor design CW WFFSM. As presented in Fig. 14, Although the modular rotor design results in an 8% reduction in output torque, it achieves a significant 35% decrease in copper losses and a 21% reduction in core losses, leading to a 2% increase in efficiency.

IV. Comparison of Proposed and Conventional Rotor WFFSMs

For convenience, Table 2 provides a comprehensive summary of the electromagnetic performance aspects of all WFFSMs with various winding configurations and rotor topologies. This table outlines metrics such as torque, cogging torque, torque ripple, voltage THD, copper and core loss, efficiency at rated conditions, and manufacturing considerations. The modular rotor TW WFFSM shows the highest efficiency among four different machines. This machine has the benefits of short end-winding with no winding overlap with a higher filling factor. It also provides better cooling because field and armature windings are directly accessible in the stator housing with a cooling jacket. With advanced winding cooling techniques, modular rotor TW WFFSM can reach higher output torque by pushing field and armature current densities.

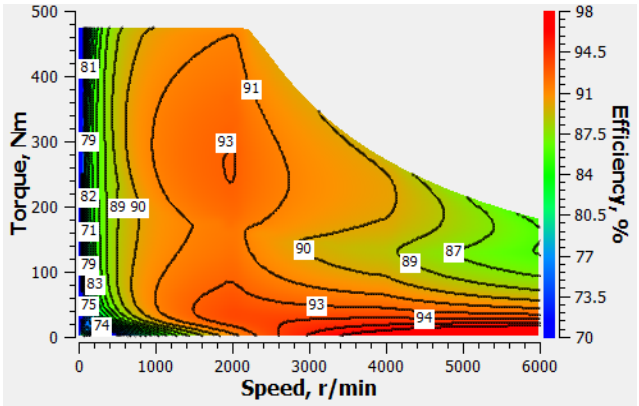

Fig. 15. Modular rotor TW WFFSM efficiency map.

Additionally, within the stator core of the TW WFFSM, the outer poles do not play a significant role in electromagnetic performance. Consequently, keeping the same outer diameter makes it possible to remove these outer poles in the stator and push the stator yoke outward, thus providing additional space for accommodating more field and armature windings (higher N_{dc} and N_{ac}). It is evident that this approach further reduces the stator core loss.

The efficiency map of the modular rotor TW WFFSM is plotted in Fig. 15. Notably, the WFFSMs possess a field regulation capability, enabling them to maintain significantly better efficiency in the constant power region, particularly at very low torque and high-speed conditions. The spider graphs comparing the normalized electromagnetic performance of toothed and modular rotors for TW WFFSM and CW WFFSM are presented in Fig. 16 and 17. The modular rotor design enhances all electromagnetic performance metrics of TW WFFSM by increasing torque and efficiency while reducing core loss and voltage THD. For CW WFFSM, it improves efficiency but decreases output torque and voltage THD.

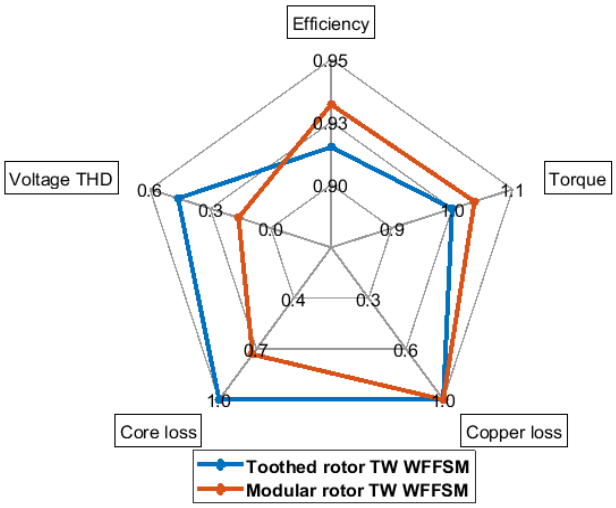

Fig. 16. Toothed and modular rotor TW WFFSM normalized electromagnetic performance comparison.

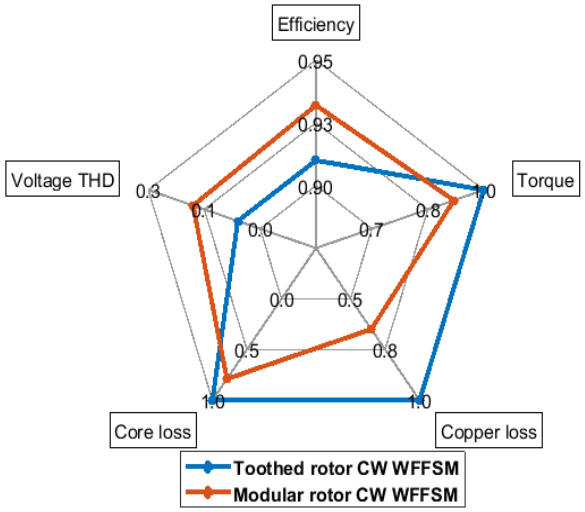

Fig. 17. Toothed and modular rotor CW WFFSM normalized electromagnetic performance comparison.

V. Conclusion

Wound-field flux-switching machines provide several attractive features such as simple rotor structure, efficient thermal management, and field regulation. However, there is more room for improvement in rotor design to enhance the electromagnetic performance, including torque, ripple torque, and efficiency. A new modular rotor design is proposed to enhance the electromagnetic performance of WFFSMs. A comprehensive core loss and torque analysis is carried out to investigate the impact of modular rotor design on torque, core loss, and efficiency. The modular rotor topology offers significant reductions in core loss while simultaneously enhancing torque and efficiency.

References

[1] "Reduced rare earth and magnet-free motors," *E-Mobility Engineering*, Apr. 25, 2023. https://www.emobility-engineering.com/reduced-rare-earth-and-magnet-free-motors/

[2] M. Fereydoonian, K. Lee, D. Bobba, and W. Lee, "Comparative analysis of wound-field flux-switching machines with different field and armature winding configurations," *in proc. 2022 IEEE Transp. Electrific. Conf. & Expo. (ITEC), 2022, pp. 1076-1081.*

[3] M. Fereydoonian, D. Bobba, and W. Lee, "Magnetic flux path and inductance analysis of flux-switching machines with different field and armature winding configurations," in *Proc. IEEE Energy Convers. Cong. and Expo. (ECCE)*, 2022, pp. 1-6.

[4] L. R. Huang, J. H. Feng, S. Y. Guo, Y. F. Li, J. X. Shi and Z. Q. Zhu, "Rotor Shaping Method for Torque Ripple Mitigation in Variable Flux Reluctance Machines," in *IEEE Transactions on Energy Conversion*, vol. 33, no. 3, pp. 1579-1589, Sept. 2018.

[5] A. Zulu, "Flux switching machines using segmental rotors," Ph.D. dissertation, School of Elec. Electron. and Comput. Eng., Newcastle Univ., Newcastle, UK, 2010.

[6] Y. Tang, E. Ilhan, J. H. Paulides and E. A. Lomonova, "Design considerations of flux-switching machines with permanent magnet or DC excitation," *15th Eur. Conf. on Power Electron. and Appl.* (EPE), Lille, France, 2013, pp. 1-10.

[7] M. Ibrahim and P. Pillay, "Aligning the Reluctance and Magnet Torque in Permanent Magnet Synchronous Motors for Improved Performance," *2018 IEEE Energy Conversion Congress and Exposition (ECCE)*, Portland, OR, USA, 2018, pp. 2286-2291.

[8] Z. Q. Zhu and Y. Xiao, "Novel Magnetic-Field-Shifting Techniques in Asymmetric Rotor Pole Interior PM Machines With Enhanced Torque Density," in *IEEE Transactions on Magnetics*, vol. 58, no. 2, pp. 1-10, Feb. 2022, Art no. 8100610.

[9] S. Saeidabadi, L. Parsa, K. Corzine, C. Kovacs and T. J. Haugan, "A Double Rotor Flux Switching Machine With HTS Field Coils for All Electric Aircraft Applications," in *IEEE Transactions on Applied Superconductivity*, vol. 33, no. 5, pp. 1-7, Aug. 2023, Art no. 5203107.

[10] M. Fereydoonian, K. Lee, G. Choi, and W. Lee, "Rotor Saliency Optimization for High-Power Density Wound-Field Flux-Switching Machines," *in Proc. IEEE Energy Convers. Cong. and Expo. (ECCE)*, Nashville, TN, USA, 2023, pp. 3867-3874.

[11] A. Lindner and I. Hahn, "Simulation of a toroidal wound flux-switching permanent magnet machine," *IECON 2014 - 40th Annu. Conf. of the IEEE Ind. Electron. Soc.,* 2014.

[12] M. Liu, Y. Li and B. Sarlioglu, "Thermal analysis of a novel dual-stator 6/4 flux-switching permanent magnet machine," 2017 *IEEE Power & Energy Society General Meeting*, Chicago, IL, USA, 2017, pp. 1-5.